

## Accepted Manuscript

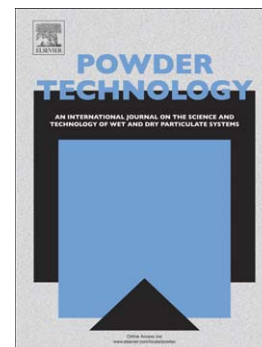
Study of the uniaxial cold compaction of AISI 316L stainless steel powders through single action tests

I. Cristofolini, A. Molinari, G. Pederzini, A. Rambelli

PII: S0032-5910(16)30138-3  
DOI: doi: [10.1016/j.powtec.2016.03.045](https://doi.org/10.1016/j.powtec.2016.03.045)  
Reference: PTEC 11577

To appear in: *Powder Technology*

Received date: 19 November 2015  
Revised date: 25 February 2016  
Accepted date: 23 March 2016



Please cite this article as: I. Cristofolini, A. Molinari, G. Pederzini, A. Rambelli, Study of the uniaxial cold compaction of AISI 316L stainless steel powders through single action tests, *Powder Technology* (2016), doi: [10.1016/j.powtec.2016.03.045](https://doi.org/10.1016/j.powtec.2016.03.045)

This is a PDF file of an unedited manuscript that has been accepted for publication. As a service to our customers we are providing this early version of the manuscript. The manuscript will undergo copyediting, typesetting, and review of the resulting proof before it is published in its final form. Please note that during the production process errors may be discovered which could affect the content, and all legal disclaimers that apply to the journal pertain.

Study of the uniaxial cold compaction of AISI 316L stainless steel powders through single action tests

I. Cristofolini<sup>a</sup>, A. Molinari<sup>a</sup>, G. Pederzini<sup>b</sup>, A. Rambelli<sup>b</sup>

<sup>a</sup> Department of Industrial Engineering - DII, Via Sommarive 9, 38123, Trento, Italy

<sup>b</sup> Technical Department (Special Pressing) - Sacmi Imola S.C., Via Provinciale Selice 17/a – 40026 Imola (BO) - Italy

**corresponding author**

**prof. Alberto Molinari**

**Department of Industrial Engineering, University of Trento**

**Via Sommarive 9, 38123 Trento (Italy)**

**Tel. +393486081199**

**Email [alberto.molinari@unitn.it](mailto:alberto.molinari@unitn.it)**

**Abstract**

The behavior during uniaxial cold compaction of a commercial mix of a water atomized austenitic stainless steel powder and a lubricant was investigated by carrying out single action tests and recording the force applied by the upper punch to the powder column, the force applied to the die, and the displacements of the crosshead and of the die. Data collected during the experiments were elaborated using different correlations between the axial stress and the radial stress in the powder column: the Poisson correlation for the elastic deformation of the powder column, and the Von Mises criterion for plastic deformation.

Friction coefficient decreases on increasing relative density up to  $\rho_r=0.7$ , then it stabilizes on 0.15. The flow stress of the powder mix increases with the relative density by a power law. The radial stress transmission coefficient increases with relative density, with two distinct trends in the ranges where either elastic or plastic deformation of the powder column predominate.

Keywords: Metal powder compaction; compaction mechanics

## Introduction

In the press-and-sinter powder metallurgy process, powders are first uniaxially cold compacted in rigid dies, to obtain the so-called green part that is further sintered to form the metallic bonding between the powder particles. Apart from specific products as, for instance, filters and self-lubricating bearings where residual porosity is the main functional characteristic, cold compaction aims at obtaining the maximum green density compatible with the geometrical complexity of the part. Densification during cold compaction is affected by the compressibility of the powder that depends on its chemical composition, alloying method, interstitial content, size distribution and shape, as well as on the lubricant admixed to reduce the friction between the powder and the die surface [1].

Such a friction causes a decrease of the compaction force in the powder column along the distance from the compaction surfaces, i.e. the surfaces in contact with the punches, and a consequent inhomogeneous axial distribution of green density along the height of the green part [2]. The friction coefficient between the powder and the die surface is in principle unknown, due to the particular nature of the material being compacted. The real contact surface between the powder column and the die surface changes on increasing density, due to the deformation of the particles. Moreover, lubricant is solid at the beginning, and then it melts due to the frictional heat spreading over the interparticle spaces. Its efficiency increases during compaction. The friction coefficient has been subject of investigation by several authors. Al Quareshi et al. [3, 4] compared the results of a theoretical analysis of cold compaction to experimental data, determining such a coefficient that was assumed as constant during the compaction cycle. Mosbah et al. [5] determined the friction coefficient versus the relative density for an iron powder in a hardmetal die in case of die wall lubrication, obtaining a constant value up to 0.7 relative density, followed by a continuous decrease. A continuous decrease over the whole relative density range is instead reported by Wikman et al. [6, 7], while Pavier and Doremus [8] propose a dependence on the normal stress that confirms the variation with density.

Uniaxial compaction in rigid dies actually occurs under a triaxial state of stress, due to the constrain exerted by the die against the expansion of the powder column in the compaction plane. For instance, in the simple case of an axialsymmetric part, the densification of the powder column is the result of its reaction to the axial stress applied by the punches, and to the radial and tangential stresses exerted by the die. The radial stress  $\sigma_r$  depends on the axial one  $\sigma_a$  through the radial stress transmission coefficient  $K$  ( $= \sigma_r/\sigma_a$ ), which is a function of the actual density during compaction, and such a dependence is an inherent characteristic of the powder [5, 7], mainly correlated to the

interparticle friction. Therefore,  $K$  depends on the particle size and shape, as well as on the lubricant admixed.

The knowledge of the friction coefficient and of the radial stress is needed to describe cold compaction, the densification behaviour of the powder and the mechanics of the process [9]. The friction coefficient may be determined by measuring the force transmitted by the powder column to the lower punch [10]. A comparative study of different experimental methods was carried out in the frame of the PM Modnet project [11]. The radial stress can be measured either through load cells in the die or through strain gauges on the outer surface of the die. Friction between the powder column and the die surface may be determined by measuring the force transmitted to the lower punch by the powder column.

In the present work, an alternative method is experimented to determine the two variables, using an industrial hydraulic press, without any additional instrument and device. The method is based on the measure of the force applied to the die, along with the force applied by the upper punch and the displacements of the crosshead and of the die, which are continuously recorded.

### **Experimental procedure**

A commercial water atomised austenitic stainless powder - AISI 316L – was used to produce green parts with two different H/D ratios: 0.5 and 1,  $6.7 \text{ g/cm}^3$  density, by means of a 200 tons hydraulic press, equipped with 9 hydraulic and 1 electric closed-loop controlled axes. The diameter of the die cavity was measured by a CMM on six positions along its height, resulting  $35,004 \pm 0,003 \text{ mm}$ .

Compaction speed was 15 mm/s.

Three different compaction strategies were performed:

- a) double action realized by moving the die downwards with half a speed of the upper punch;
- b) downwards single action, realized by keeping the die still;
- c) upwards single action, realized by moving the die downwards at the same speed as the upper punch.

The following data were recorded:

- )  $F$ , the compaction force, i.e. the force applied to the crosshead (related to the force applied to the powder column by the upper punch);
- )  $F_d$ , the die force, i.e. the force to move the die according to the different compaction strategies;
- )  $X$ , the position of the lower surface of the upper punch with respect to the upper surface of the lower punch (as derived from the distance measured by two encoders fixed to the crosshead and to the base plate of the press, respectively);

- )  $Z$ , the position of the upper surface of the die, again with respect to the upper surface of the lower punch (as derived from the distance measured by two encoders fixed to the die and to the base plate of the press, respectively).

Figure 1 shows, as an example, the data recorded during the whole compaction cycle versus time in case of the downwards single action test to produce the  $H/D=1$  green part.  $Z$  is set constant during the whole compaction step. A positive value of  $F$  is representative of a downward force, while a positive value of  $F_d$  is representative of an upwards force. A detail of the first part of the cycle is reported to highlight the contribution of the weight of the compaction tools and of the die to the relevant forces.

*Figure 1: Forces and displacements versus time as recorded by the press*

When the crosshead moves downwards to approach the powder, a negative (upwards) force of about 5 kN is recorded. Since the crosshead moves at a constant speed, this force represents a portion of its weight, which is not compensated and has to be added to the recorded force to calculate the effective compaction force. Moreover, a positive (upwards) force of about 9 kN is recorded when the die is kept still; it represents the weight of the die that has to be added to the recorded  $F_d$ . These corrections were applied to all the data collected.

## Results and discussion

Figure 2 shows the record of  $F$ ,  $F_d$ ,  $X$  and  $Z$  during cold compaction to produce the specimen with  $H/D = 0.5$  with the three strategies. Some downshooting of  $X$  may be observed in double action and, slightly more pronounced, in downwards compaction (highlighted by the frame around the record of  $X$  in the figure); consequently, the record of  $F$  shows a maximum and then a slight decrease up to the end of the compaction step. A sharp decrease in force characterizes unloading, being both  $X$  and  $Z$  nearly still. Ejection is carried out by moving  $Z$  downwards and maintaining a hold-down force of about 100 kN on the powder column.

*Fig. 2: forces and displacements recorded by the press in the three different compaction strategies –  $H/D$  0.5*

The compaction force is applied to the powder column by both the upper and the lower punches. To describe the mechanics of compaction, the two forces are considered in the following, defined as  $F_u$

(upper punch) and  $F_l$  (lower punch), the former being equal to  $F$ . Figure 3 shows  $F_u$  which allows obtaining the same green density with the three different strategies.

*Fig. 3: Force to obtain the same green density for both H/D ratios in the three different compaction strategies*

In double action,  $F_u$  increases slightly with H/D, as expected, due to the larger axial gradient that reduces the mean compaction force along the height of the powder column. In downwards compaction, the axial gradient is larger than in double action;  $F_u$  to achieve the same green density is consequently higher and its increase with H/D is more pronounced. The compaction force applied by the upper punch in upwards compaction is the lowest, and slightly decreases on increasing H/D. Contrary to the previous cases, the frictional forces on the powder column are directed downwards, contributing to densification; the force applied by the upper punch is therefore lower and decreases on increasing H/D, since frictional force increases. Due to the different contribution of the frictional forces to compaction, the force applied by the lower punch  $F_l$  is lower than  $F_u$  in downwards compaction, and higher than  $F_u$  in upwards compaction.

Figure 2 shows that  $F_d$  is constant during the double action compaction step while in the other cases it increases continuously, either up or downwards. A positive value of  $F_d$  is indicative of an upwards force, a negative value of a downwards force. To understand the different trends of  $F_d$  in the three compaction strategies, reference has to be made to figure 4 where the forces applied by the upper and the lower punches to the powder column, and the forces acting on the die during the three different cold compaction strategies are shown.

*Figure 4: Scheme of forces distribution in the three different compaction strategies*

In double action compaction, the relative displacement of the upper half of the powder column to the die is directed downwards, while that of the lower half is upwards, thus resulting in an inversion of the direction of the frictional force  $F_{\square}$  transmitted to the die. In downwards and upwards compaction the relative displacement of the powder column and the resulting frictional forces are directed downwards and upwards, respectively, along the whole of the die cavity surface. The frictional forces have therefore a finite global effect on the die. During downwards compaction, the increase in the axial force increases the radial one and, in turn, the frictional force; a continuously increasing upwards force has to be applied to the die to keep it still. On the contrary, during

upwards compaction the frictional force opposes the movement of the die and a continuously increasing downwards force has to be applied to maintain its velocity constant.

In case of perfect double action, the axial gradients of the compaction force and of the radial force  $F_r$  are symmetric with respect to the median cross section. The global effect of frictional forces  $F_{\mu}$  on the die is expected to be zero, as actually observed during the compaction test, where  $F_d$  is constant (equal to zero) during the whole compaction step.

Eq. (1) expresses the equilibrium of the forces acting on the die

$$F_d + F_{\mu} = 0 \quad (1)$$

Where  $F_{\mu}$  is the mean frictional force along the die cavity surface. Figure 5 shows  $F_{\mu}$  vs.  $F_u$  in the two uniaxial compaction strategies for both H/D ratios; since the frictional force is proportional to the extension of the friction surface, in the compaction of H/D=1 specimens the frictional force is twice the force needed in the compaction of the H/D=0,5 ones.

*Fig. 5: Frictional force versus force applied by the upper punch for the two uniaxial compaction strategies – both H/D ratios*

Eq. (2) correlates the mean frictional force to the mean radial force  $F_r$  and to the mean radial stress  $\sigma_r$ .

$$F_{\mu} = \mu \cdot F_r = \mu \cdot \sigma_r \cdot S \quad (2)$$

$\mu$  is the friction coefficient between the powder column and the internal surface of the die and  $S$  is the extension of the friction surface, given by eq. (3)

$$S = \pi \cdot D \cdot h \quad (3)$$

where  $D$  is the diameter of the die cavity and  $h$  the actual height of the powder column.  $h$  was determined by the position  $X$  of the upper punch, to which the elastic displacement of the tools, measured using specimens the stiffness of which is known, was added [12, 13].

Figure 6 shows the resulting mean radial stress  $\sigma_r$  multiplied by the friction coefficient  $\mu$ , calculated from  $F_{\mu}$  combining equations (2) and (3), as a function of the axial stress applied by the upper punch  $\sigma_{a,u}$ , given by eq. (4).

$$\sigma_{a,u} = F_u \cdot \pi \cdot \frac{D^2}{4} \quad (4)$$

*Fig. 6:  $\mu \sigma_r$  versus  $\sigma_{a,u}$  for the two uniaxial compaction strategies – both H/D ratios*

Since  $\sigma_{a,u}$  is not the mean axial stress in the powder column, the curves do not represent the radial vs. axial stress diagram from which the yield condition and the flow stress of the material can be calculated. The mean axial stress depends on the gradient of the axial force in the powder column, and can be calculated as follows.

First, the force applied by the powder column to the lower punch ( $= -F_l$ ) is calculated from the equilibrium of the forces acting on the powder column, which are shown in figure 7.

*Fig. 7: scheme of the forces acting on the powder column in the two uniaxial compaction strategies*

Neglecting the sliding occurring among the powder particles close to the die surface at low density, when the shear strength of the material is quite low [7], the equilibrium of the forces is expressed by equations (5) and (6) for downwards and upwards compaction, respectively.

$$F_u = F_\mu + F_l \quad (5)$$

$$F_u + F_\mu = F_l \quad (6)$$

Figure 8 shows the correlation between  $F_u$  and  $F_l$  during the whole of the compaction step.

*Fig. 8: force applied by the lower punch versus force applied by the upper punch for the two uniaxial compaction strategies – both H/D ratios*

The mean axial stress  $\sigma_a$  can now be calculated from the equation of the axial gradient of the compaction force [2]:

$$F_x = F_u \cdot e^{-4\mu \frac{\sigma_r \cdot x}{\sigma_a D}} \quad (7)$$

$F_x$  is the axial force at a distance  $x$  from the upper surface,  $\sigma_r$  and  $\sigma_a$  are the mean radial and the mean axial stress, respectively, and  $D$  is the diameter of the powder column, i.e. the diameter of the die cavity. If  $h$  is the actual height of the powder column corresponding to  $F_u$  and  $F_l$ , eq. (7) becomes eq. (8) for downwards compaction and eq. (9) for upwards compaction.

$$F_l = F_u \cdot e^{-4\mu \frac{\sigma_r \cdot h}{\sigma_a D}} \quad (8)$$

$$F_l = F_u \cdot e^{4\mu \frac{\sigma_r \cdot h}{\sigma_a D}} \quad (9)$$

The mean axial stress is the only unknown value, since the product  $\sigma_r \sigma_a$  is known from eq. (2) and (3); it may be therefore calculated from equations (10) and (11) for downwards and upwards compaction, respectively:

$$\sigma_a = \frac{-4 \cdot \mu \sigma_r \cdot h}{D \cdot \ln \frac{F_l}{F_u}} \quad (10)$$

$$\sigma_a = \frac{4 \cdot \mu \sigma_r \cdot h}{D \cdot \ln \frac{F_l}{F_u}} \quad (11)$$

Figure 9 shows the mean radial stress multiplied by the friction coefficient vs. the mean axial stress.

*Fig. 9:  $\mu \sigma_r$  versus  $\sigma_a$  for the two uniaxial compaction strategies – both H/D ratios*

The friction coefficient during the compaction experiments may be determined considering the phenomena occurring during cold compaction of the powder and the relevant theoretical correlations between the radial and the axial stress. Densification of the powder column during the loading step of cold compaction occurs by three mechanisms: rearrangement, elastic deformation and plastic deformation. Elastic deformation is recovered on unloading, and densification results from rearrangement and plastic deformation. Rearrangement is due to the relative movement of the particles promoted by the application of the compaction force and leads to an increase in packing. It mostly occurs in the early stage of compaction, since the continuous increase in density tends to impede such a relative movement. Fracture and fragmentation of the powder particles might further induce rearrangement, but these phenomena are unlikely in ductile metallic powders. Densification is therefore due to rearrangement in the low compaction force range, and to plastic deformation of the powder column in the medium-high force range.

The correlation between radial and axial stress at the lower compaction forces, where the powder is subject to elastic deformation, is given by equation (12)

$$\sigma_r = \sigma_a \cdot \frac{\nu}{1-\nu} \quad (12)$$

where  $\nu$  is the Poisson coefficient of the powder.

In the medium/high range of force, where plastic deformation predominates, the correlation is expressed by the plasticity criterion. Several plastic models have been developed for cold compaction. Some of them (Shima, Fleck and CamClay models) have been subject of a comparative analysis for the modelling of metallic powders by Sun et al. [14]. Another comparative study was carried out in the frame of the PM Modnet project coordinated by EPMA [9], where the cold compaction of a real part was simulated by different research centers with different models, and verified experimentally. Recently, Rolland et al. used a modified CamClay model to evaluate the effect of the Lode dependency in the cold compaction process [15]. A detailed analysis of the

different models is out of the scope of the present investigation. Therefore, in a first approach, the Von Mises criterion, used by Al Quareshi et al. [3, 4], is adopted. In the analysis of a disk shaped part using cylindrical coordinates, such a criterion is expressed by eq. (13).

$$\sigma_a = \sigma_r + \sigma_f \quad (13)$$

$\sigma_f$  is the flow stress of the powder that increases continuously during compaction due to densification and strain hardening. The dependence of  $\sigma_f$  on density is a characteristic of the powder.

The main problem is defining either the force or the relative density ranges where elastic and plastic deformation predominate. In a previous work [12], the boundary between the two ranges in double action cold compaction of the same powder was individuated in correspondence of an upper axial stress  $\sigma_{a,u}$  around 200 MPa. It corresponds to a mean axial stress of 180-190 MPa in single action compaction. Figure 10 shows the relative density  $\rho_r$  versus the mean axial stress for the two uniaxial compaction strategies – both H/D ratios. The relative density was calculated from the actual height of the powder column, the die diameter and the mass of the powder.

*Fig. 10: Relative density versus mean axial stress for the two uniaxial compaction strategies – both H/D ratios*

The transition from predominating elastic to predominating plastic deformation occurs at a relative density of 0.7, as highlighted by the analysis of the curves; therefore, the mean axial vs. mean radial stress correlation will be analyzed using eq. (12) below such a relative density and using eq. (13) above it.

In elastic deformation axial and radial stress are correlated through the Poisson coefficient. Just only a very few data are available in literature for the Poisson coefficient of powders. For a spherical stainless steel powder in the relative density range between 0.58 and 0.86 Carnavas and Page [16] propose  $\nu$  ranging between 0.25 and 0.20, with a minimum at 0.76 relative density. Mosbah et al. [5] determined the Poisson coefficient of an iron powder in the relative density range between 0.68 and 0.92; in this case  $\nu$  increases with relative density from 0.3 up to 0.33. A constant value of 0.3 is assumed in the present work. Eq. (12) is transformed in equation (14) simply multiplying by the friction coefficient the two terms

$$\mu\sigma_r = \mu \cdot \sigma_a \cdot \frac{\nu}{1-\nu} \quad (14)$$

So that the only unknown variable is  $\mu$ , being the term  $\mu\sigma_r$  known from experiments. The friction coefficient may be therefore calculated as

$$\mu = \frac{\mu\sigma_r \cdot (1 - \nu)}{\sigma_a \cdot \nu} \quad (15)$$

Figure 11 shows the calculated friction coefficient as a function of relative density in the 0.4-0.7 range.

*Fig. 11: Calculated friction coefficient versus relative density for the two uniaxial compaction strategies – both H/D ratios*

The graphs show quite a large instability of  $\mu$  at the beginning of the compaction cycle (due to the scatter of  $F$  and  $F_d$  around quite small values), followed by a gradual decrease down to 0.17-0.2 at 0.7 relative density. This trend agrees with the results of Wikman et al. [6, 7] and of Pavier and Doremus [8]. The  $\mu$  vs. relative density relationship is not expected to depend on the compaction strategy, being mostly dependent on the powder mix and the roughness of the die cavity surface. The empirical relationship between friction coefficient and relative density given by eq. (16) was calculated by fitting the averaged data.

$$\mu = 0.077 \cdot \rho_r^{-1.87} \quad (16)$$

Knowing  $\mu$  it is possible to calculate the mean radial stress in the range of the relative density between 0.4 and 0.7.

In the relative density range of plastic deformation (relative density above 0.7) the flow stress is given by the difference between the mean axial and the mean radial stresses, as in eq. (17).

$$\sigma_f = \sigma_a - \sigma_r \quad (17)$$

The mean axial stress in downwards and upwards compaction is given by eq. (10) and (11), respectively. The mean radial stress may be obtained by combining eq. (2) and eq. (3), resulting in eq. (18).

$$\sigma_r = \frac{F_\mu}{\mu \cdot \pi \cdot D \cdot h} \quad (18)$$

Introducing equations (10), (11) and (18) in (17), the flow stress for downwards and upwards compaction is given by eq. (19) and (20), respectively.

$$\sigma_f = -\frac{4 \cdot \mu \sigma_r \cdot h}{D \cdot \ln \frac{F_l}{F_u}} - \frac{F_\mu}{\mu \cdot \pi \cdot D \cdot h} \quad (19)$$

$$\sigma_f = \frac{4 \cdot \mu \sigma_r \cdot h}{D \cdot \ln \frac{F_l}{F_u}} - \frac{F_\mu}{\mu \cdot \pi \cdot D \cdot h} \quad (20)$$

The flow stress was calculated introducing different values of  $\mu$ ; the results are shown in figure 12, along with the equations fitting the curves. The result of calculation with  $\mu=0.1$  is not reported, since the flow stress curve shows a maximum at about 0.8 relative density, that is definitely meaningless.

*Fig. 12: Flow stress versus relative density under the hypothesis of different friction coefficient for the two uniaxial compaction strategies – both H/D ratios*

In all the cases the curves are satisfactorily fitted by the power law equation (21)

$$\sigma_f = \sigma_{f,0} \cdot \rho_r^b \quad (21)$$

where  $\sigma_{f,0}$  is the flow stress of the powder when  $\rho_r=1$ , i.e. at the theoretical density. Despite of its purely theoretical meaning,  $\sigma_{f,0}$  does not depend on the geometry of the parts (H/D ratio) and on the compaction strategy, being something like an inherent ideal characteristics of the powder used. Figure 13 plots  $\sigma_{f,0}$  (mean value and relevant standard deviation) as a function of the friction coefficient.

*Fig. 13:  $\sigma_{f,0}$  as a function of the friction coefficient for the two uniaxial compaction strategies – both H/D ratios*

The difference between the  $\sigma_{f,0}$  values relevant to the two uniaxial compaction strategies in both H/D ratios

increases with friction coefficient; it is quite low for  $\mu=0.15$ , as shown by standard deviation. The conclusion that friction coefficient during the plastic deformation step is constant and very close to 0.15 may therefore be drawn.

The correlation between the flow stress and the relative density may be calculated by averaging the four curves in figure 12 relevant to  $\mu=0.15$ , and results as eq. (22)

$$\sigma_f = 525 \cdot \rho_r^{4.82} \quad (22)$$

Finally, figure 14 shows the friction coefficient as a function of relative density in the whole of the relative density range. The trend agrees well with that reported in [9].

*Fig. 14: Friction coefficient as a function of the relative density*

The resulting correlation between mean radial stress and mean axial stress is reported in figure 15; the four diagrams representing two uniaxial compaction strategies for both H/D ratios are very similar, as expected.

*Fig. 15: Mean axial stress versus mean radial stress for the two uniaxial compaction strategies – both H/D ratios*

The radial stress transmission coefficient  $K = \sigma_r / \sigma_a$  is calculated from the data in figure 15 and reported versus the relative density in figure 16, relevant to the whole relative density range on the left, and to the 0.6-0.85 range on the right side.

*Fig. 16: Radial stress transmission coefficient versus relative density for the two uniaxial compaction strategies – both H/D ratios*

Data are highly scattered up to 0.6 relative density, due to the scatter of the measured forces around rather small values. Such a relative density range may be reasonably neglected, because of its poor practical interest. Above  $\rho_r = 0.6$  (right side in figure), the scatter of the four diagrams is much smaller, and two distinct correlations with relative density may be calculated. In the relative density between 0.6 and 0.7, where elastic deformation of the powder column predominates, the correlation is given by eq. (24)

$$K = \frac{\sigma_r}{\sigma_a} = 0.83 \cdot \rho_r - 0.15 \quad (24)$$

While above 0.7 relative density, where plastic deformation occurs is given by eq. (25)

$$K = \frac{\sigma_r}{\sigma_a} = 1.2 \cdot \rho_r - 0.4 \quad (25)$$

In both ranges, the radial stress transmission coefficient increases with relative density, confirming the results of Mosbah et al. [5].

The correlation relevant to the elastic deformation range may be used to calculate the Poisson coefficient through eq. (26),

$$\nu = \frac{K}{1 + K} \quad (26)$$

and its dependence on relative density, obtaining the following equation

$$\nu = 0.63 \cdot \rho_r - 0.13 \quad (27)$$

From which the Poisson coefficient at 0.6 and 0.7 relative density is calculated, obtaining 0.25 and 0.31, respectively, that are in a satisfactory agreement with the value assumed at the beginning of the present elaboration (0.3).

Finally, from the radial stress transmission coefficient and the friction coefficient, the axial gradient of the force in the powder column can be calculated. In a previous work [12] Cristofolini et al. determined the correlation between the compaction pressure and density of the same powder mix of the present work

$$\rho = aP^b \quad (25)$$

Where  $P$  is the ratio between the axial force  $F_u$  and the area of the compaction surface. The density gradient can be therefore calculated for the two uniaxial compaction strategies – both H/D ratios. Figure 17 shows the density gradient, expressed by the difference between the maximum and the minimum density in the powder column, as a function of the mean density, for some selected values of  $F_u$ . Diagrams are relevant to upwards compaction, and represent the results for downwards compaction, too, since the compaction strategy influences the direction of the axial gradient but not its amplitude. Instead, the gradient depends on the H/D ratio, as expected.

*Fig. 17: Density gradient as a function of the mean density for the upwards uniaxial compaction strategy – both H/D ratios*

The gradient increases with density, and the trend shows an enhancement above  $5.5 \text{ g/cm}^3$ , corresponding to a relative density of 0.7, i.e. to the start of predominating plastic deformation of the powder column.

## Conclusions

This work investigated the behavior of a water atomized austenitic stainless steel powder in cold compaction, aiming at determining the friction coefficient between the powder column and the die wall, the radial stress transmission coefficient and the dependence of the flow stress of the material on density. Single action compaction tests were carried out, both upwards and downwards, to produce specimens with two different H/D ratios, recording the force applied by the upper punch to the powder column, the force applied to the die, and the displacements of the crosshead and of the die. In single action tests, the force applied to the die is correlated to the frictional force at the die surface, and used to calculate the radial force applied by the die to the powder column.

Data collected during the experiments were elaborated using the Poisson correlation between the axial stress and the radial stress for the elastic deformation, and the Von Mises criterion for plastic

deformation. Since friction coefficient, radial stress transmission coefficient and dependence of the flow stress from density are characteristics of the powder, they do not depend on the compaction strategy and on the geometry of the parts. These characteristics were therefore determined through the convergence of the results of the elaboration of the different experiments performed.

Friction coefficient decreases on increasing relative density up to  $\rho_r=0.7$ , then it stabilizes on 0.15. Two distinct correlations between the radial stress transmission coefficient and relative density were calculated relevant to the ranges where either elastic or plastic deformation of the powder column predominate. A power law correlation between the flow stress and relative density was calculated. All these results display trends that are in agreement with the literature. The axial density gradient in the powder column was finally calculated.

The results of the present work have a significant practical interest, since they have been obtained processing the data collected during the production of green parts using the hydraulic press in the typical conditions of the industrial production, without any additional measurement device over the standard ones. They are strictly relevant to the powder used, where the lubricant added plays a significant but at the same time unpredictable role. For this reason, any attempt to interpret the models proposed starting from the mechanical properties of the austenitic stainless steel is, on the opinion of the authors, definitely meaningless. The powder mix is indeed a strange and unique composite material, made of powders and containing not only voids, but even a large volume percentage of a lubricant that is solid at the beginning of the compaction and melts due to frictional forces. On the other side, the proposed models represent the behaviour of the powder mix used in the production of parts, and therefore has a noticeable practical interest.

Nevertheless, the elaboration may be improved. For instance, the Von Mises criterion was used to elaborate the plastic step of compaction. Other models have been developed to describe the plastic deformation of the powder as a function of the triaxial state of stress. For instance, the use of the CamClay is expected to improve the reliability of the results.

## References

1. R. K. Enneti, A. Lusin, R. M. German, S. V. Atre, Effect of lubricant on green strength, compressibility and ejection of parts in die compaction process, *Powder Technology* 233 (2013) 22-29
2. S. Turenne, C. Godere, Y. Thomas, P. E. Mongeon, Evaluation of friction conditions in powder compaction for admixed and die wall lubrication, *Powder Metallurgy* 42(3) (1999) 263-268

3. H. A. Al-Quareshi, A. Galiotto, A. N. Klein, On the mechanics of cold die compaction for powder metallurgy, *Journal of Materials Processing Technology*, 166 (2005) 135-143
4. H. A. Al-Quareshi, M. R. F. Soares, D. Hotza, M. C. Alves, A. N. Klein, Analysis of the fundamentals parameters of cold die compaction of powder metallurgy, *Journal of Materials Processing Technology*, 199 (2008) 417-424
5. P. Mosbah, D. Bouvard, E. Ouedraogo, P. Stutz, Experimental techniques for analysis of die pressing and ejection of metal powder, *Powder Metallurgy* 40(4) (1997) 269-277
6. B. Wikman, H. A. Haggblad, M. Oldenburg, Modelling of powder-wall friction for simulation of iron powder pressing, *Proceedings International Workshop on "Modelling of metal powder forming process"*, Grenoble, France, 1997, 149-157
7. B. Wikman, N. Solimannehad, R. Larsson, M. Oldenburg, H. A. Haggblad, Wall friction coefficient estimation through modelling of powder die pressing experiment, *Powder Metallurgy* 43(2) (2000) 132-138
8. E. Pavier and P. Doremus, Friction behaviour of an Iron Powder Investigated with Two Different Apparatus, *Proceedings International Workshop on "Modelling of metal powder forming process"*, Grenoble, France, 1997, 335-344
9. PM Modnet Computer Modelling Group, Comparison of computer models representing powder compaction process, *Powder Metallurgy* 42(4) (1999) 301-311
10. Y. Tien, P. Wu, W. Huang, M. Kuo, C. Chu, Wall friction measurement and compaction characteristics of bentonite powders, *Powder Technology* 173 (2007) 140-151
11. PM Modnet Methods and Measurement Group, Measurements of friction for powder compaction modelling – comparison between laboratories, *Powder Metallurgy* 43(4) (2000) 364-374
12. I. Cristofolini, A. Molinari, G. Pederzini, M. Piva, A. Grandi, From experimental data an analytical model of powder behavior during uniaxial cold compaction, *Advances in powder Metallurgy and Powder Technology* 1 (2015) 19-30
13. I. Cristofolini, A. Rambelli, G. Pederzini, A. Molinari, Densification and deformation during uniaxial cold compaction of stainless steel powder with different particle size, accepted for publication on *Powder Metallurgy*
14. X. Sun, S. Chen, J. Xu, L. Zhen, K. Kim, Analysis of cold compaction densification behaviour of metal powders, *Materials Science and Engineering A267* (1999) 43-49
15. S. A. Rolland, P. Mosbah, D. T. Gethin, R. W. Lewis, Lode dependency in the cold die powder compaction process, *Powder Technology* 221 (2012) 123-136

16. P. C. Carnavas and N. W. Page, Elastic properties of compacted metal powders, *Journal of Materials Science* 33 (1998) 4647-4655

ACCEPTED MANUSCRIPT

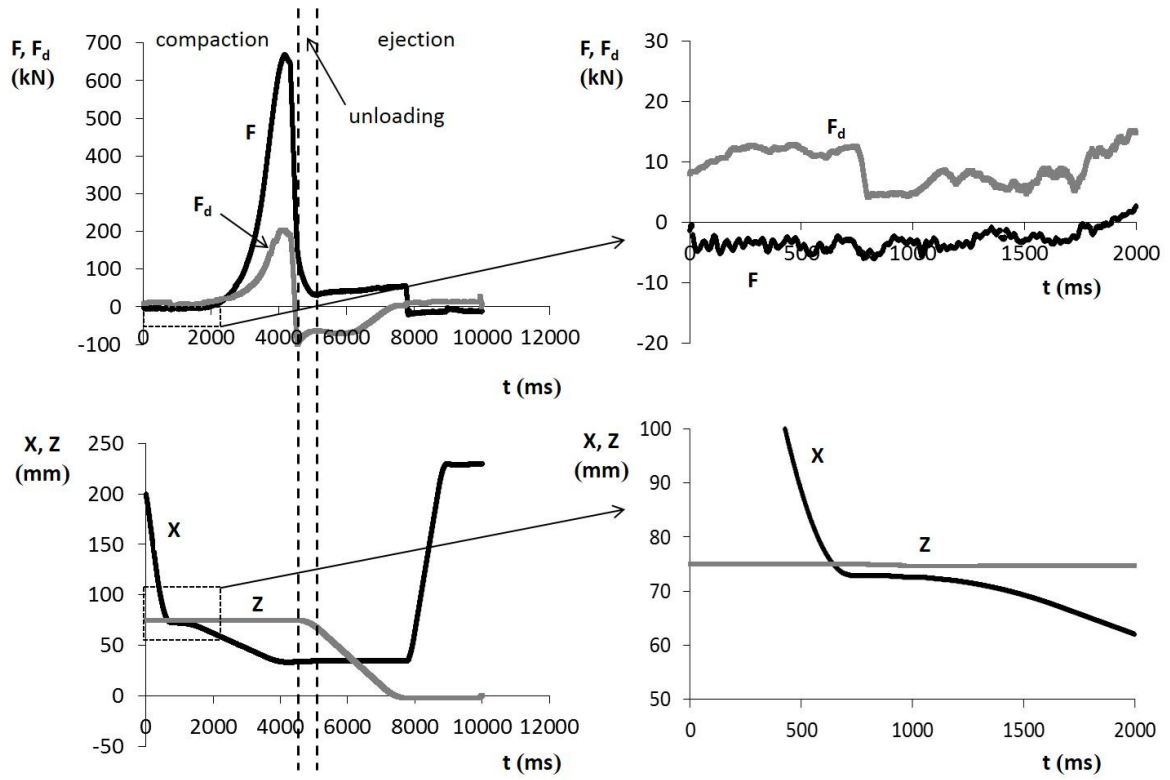


Fig. 1

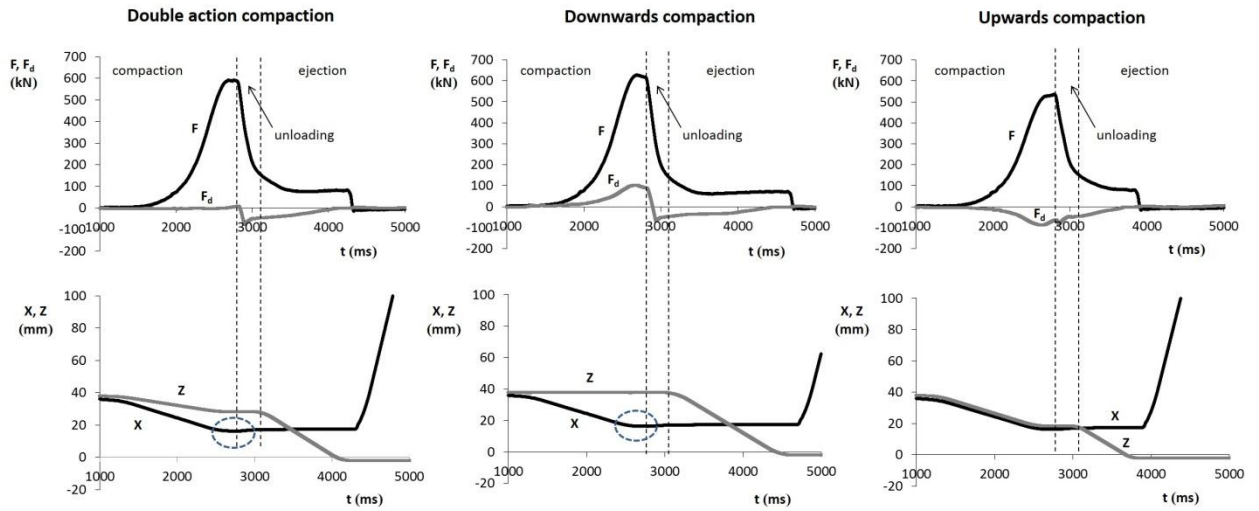


Fig. 2

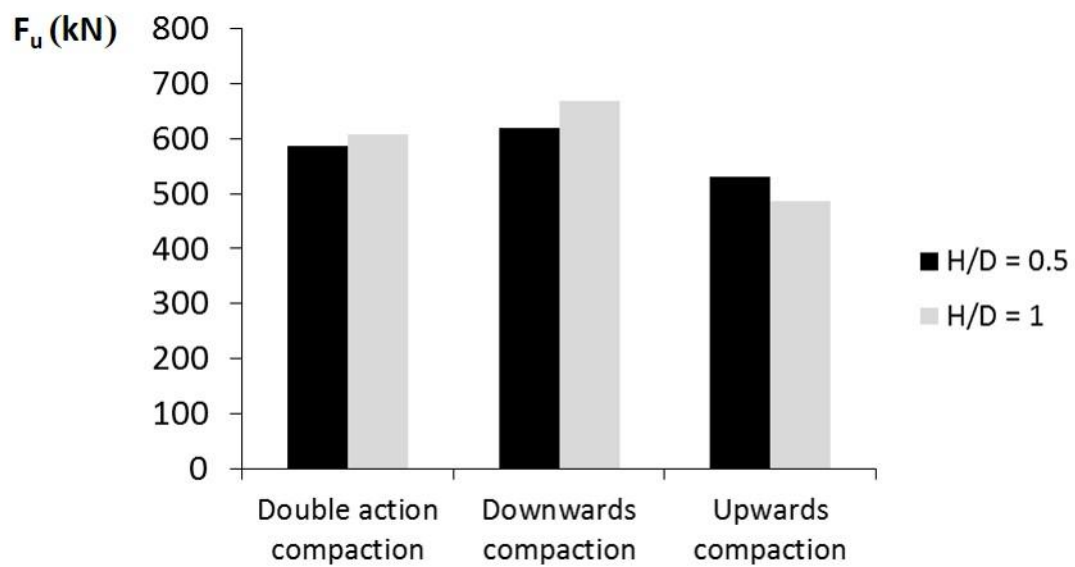


Fig. 3

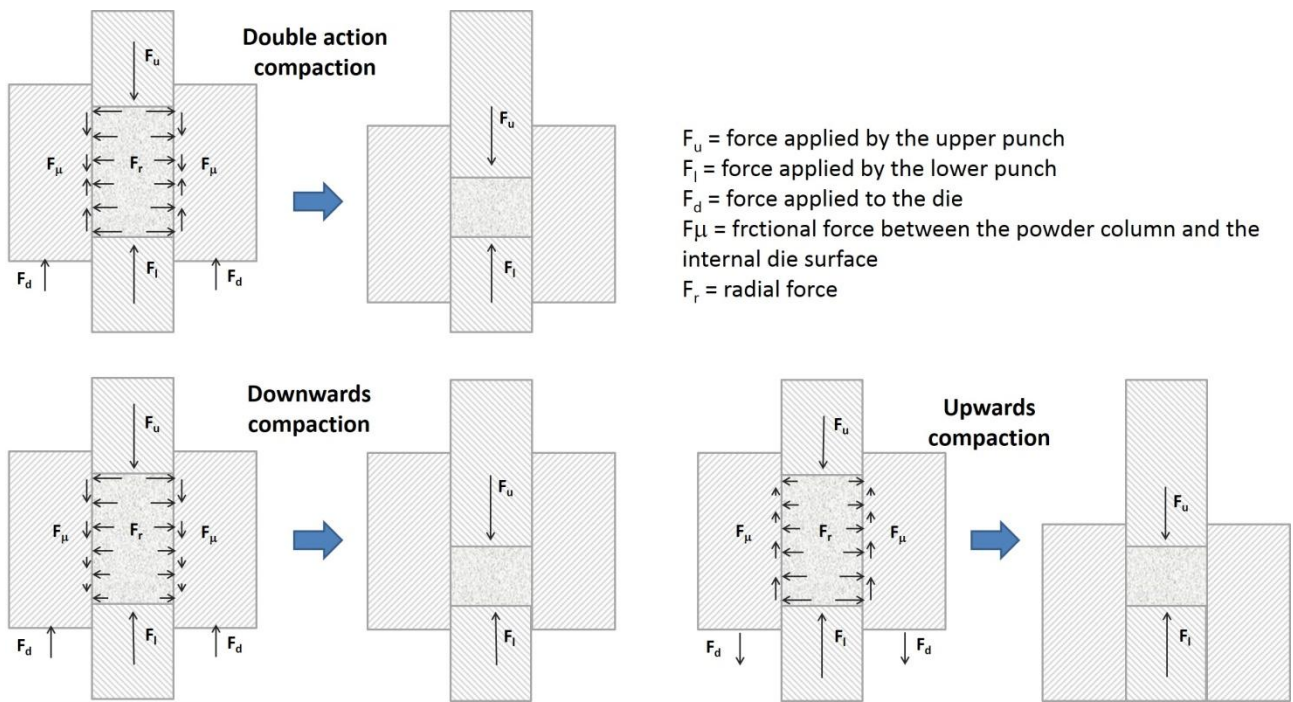


Fig. 4

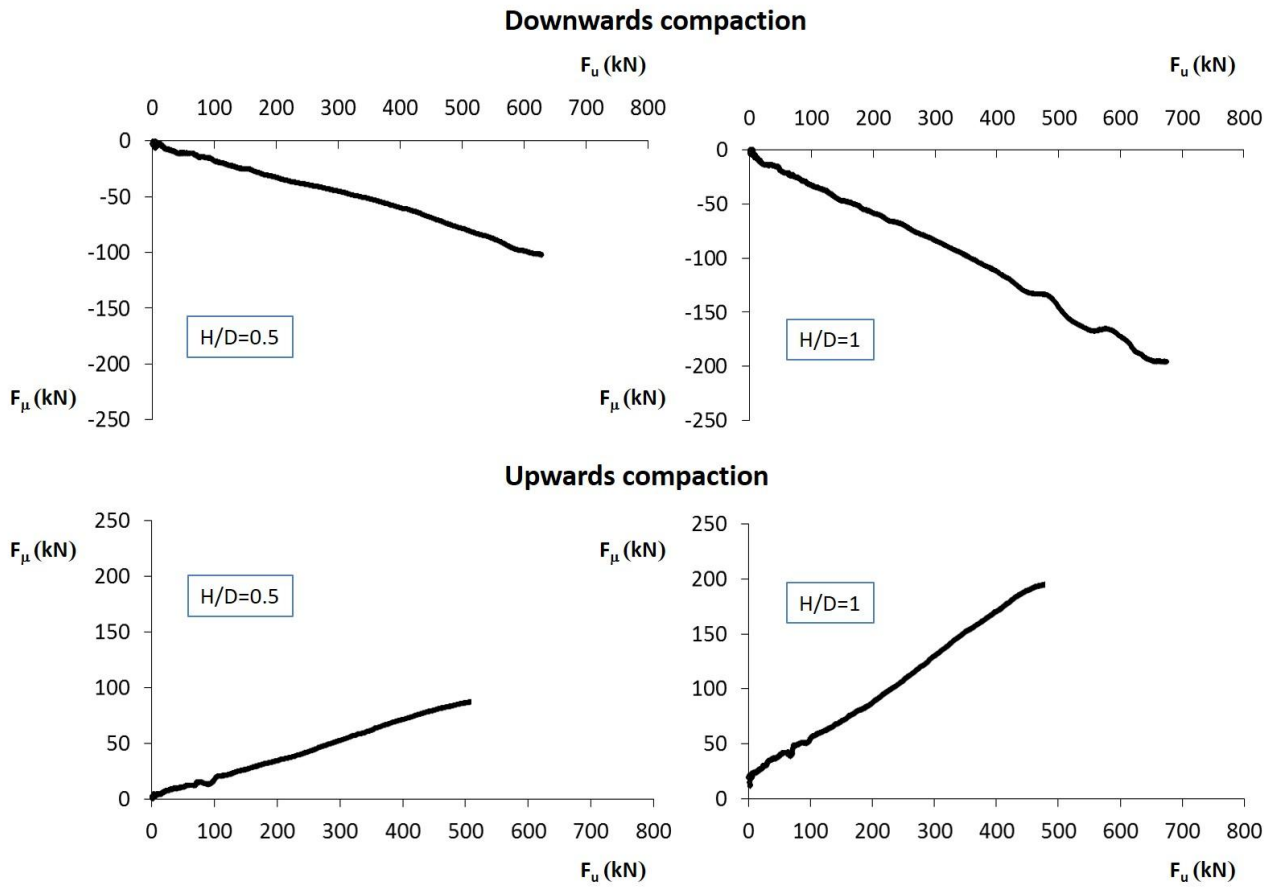


Fig. 5

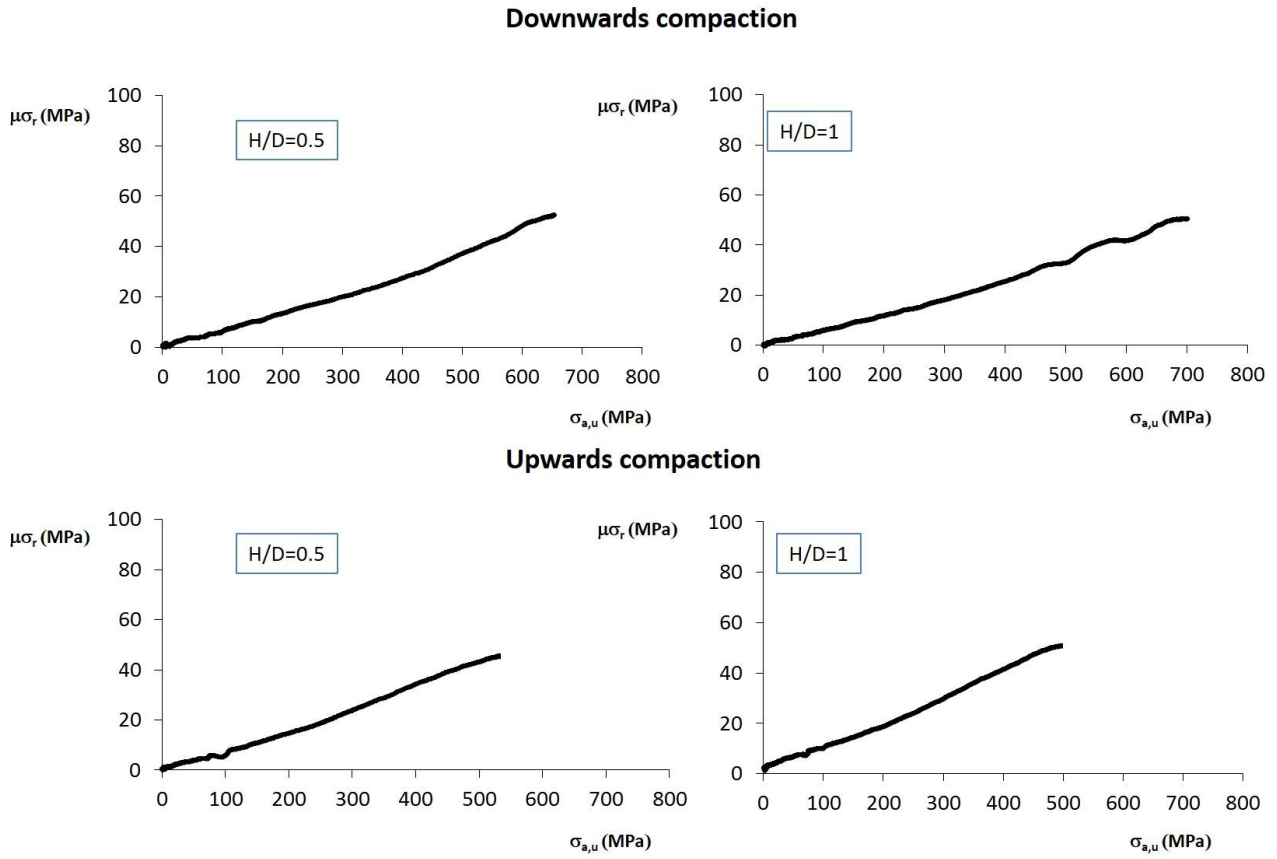


Fig. 6

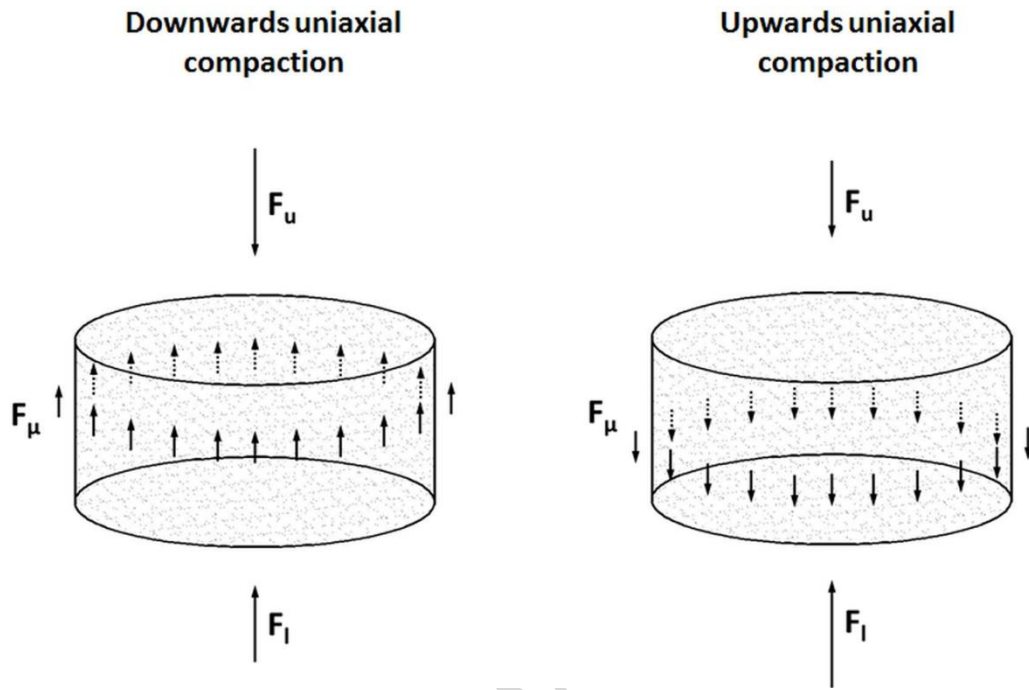


Fig. 7

ACCEPTED MANUSCRIPT

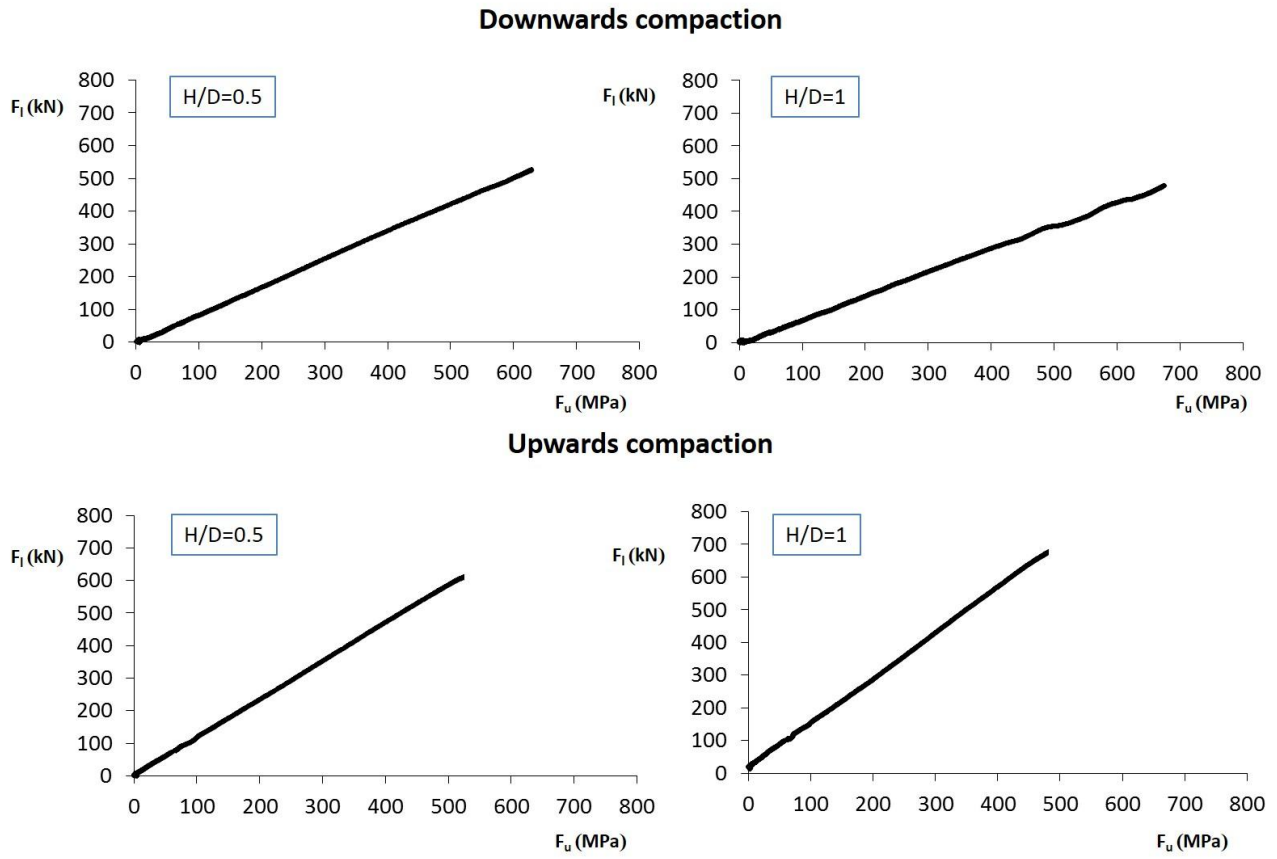


Fig. 8

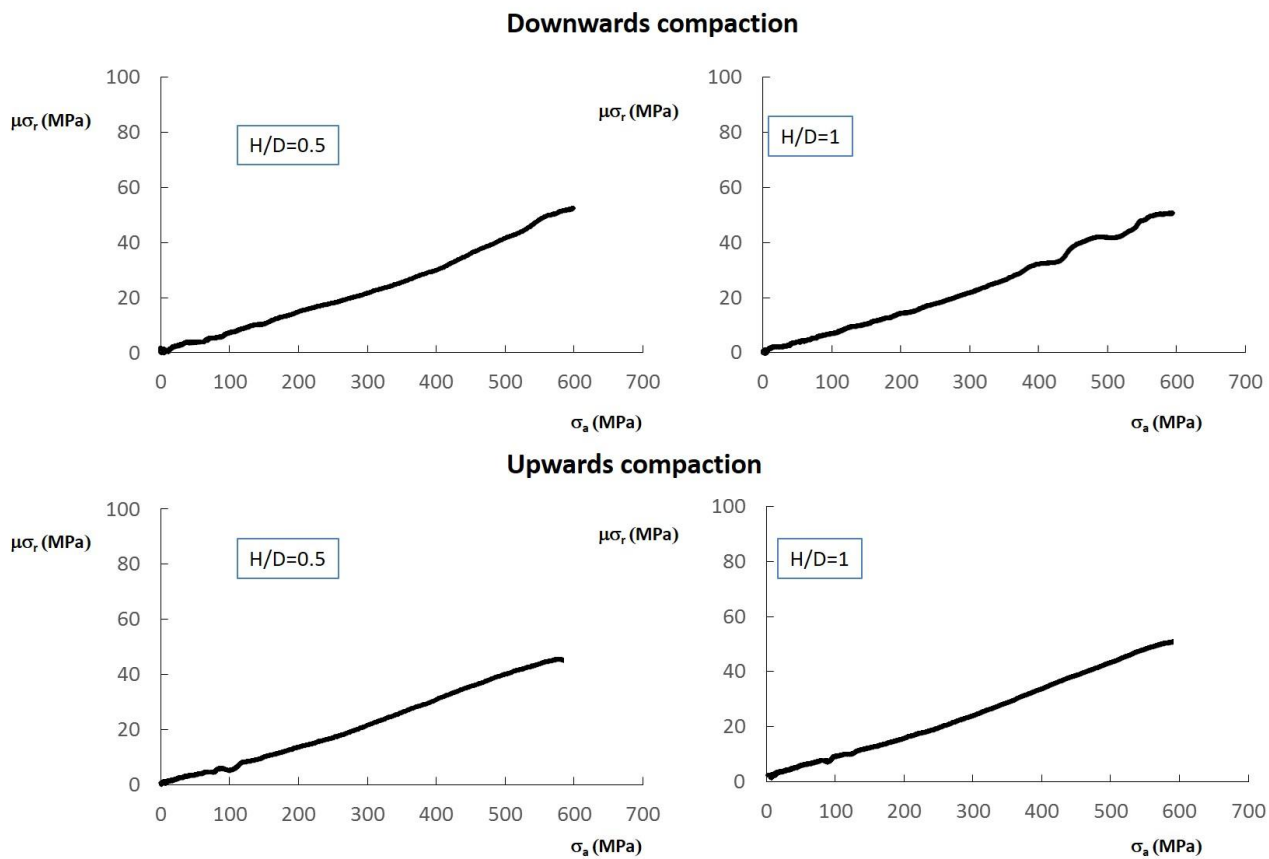


Fig. 9

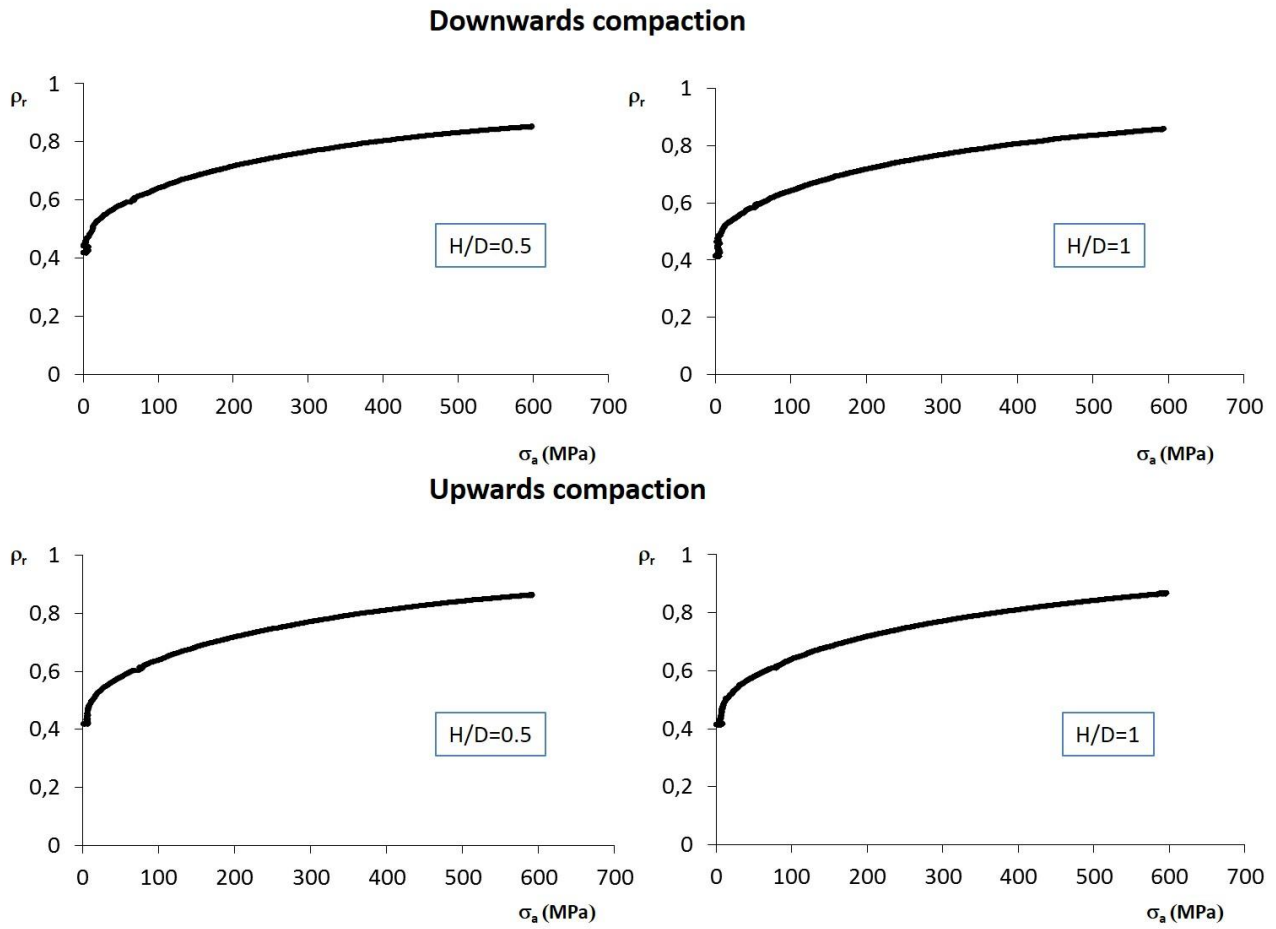


Fig. 10

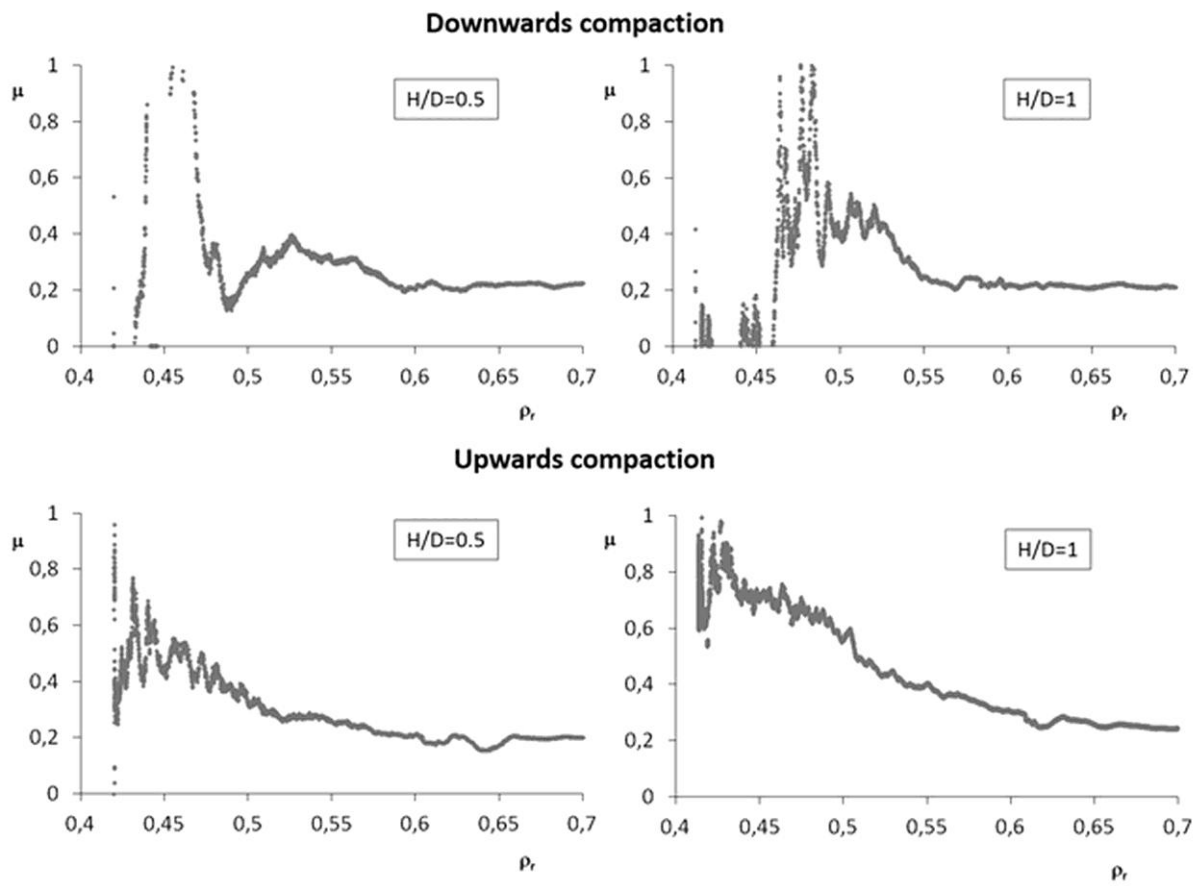


Fig. 11

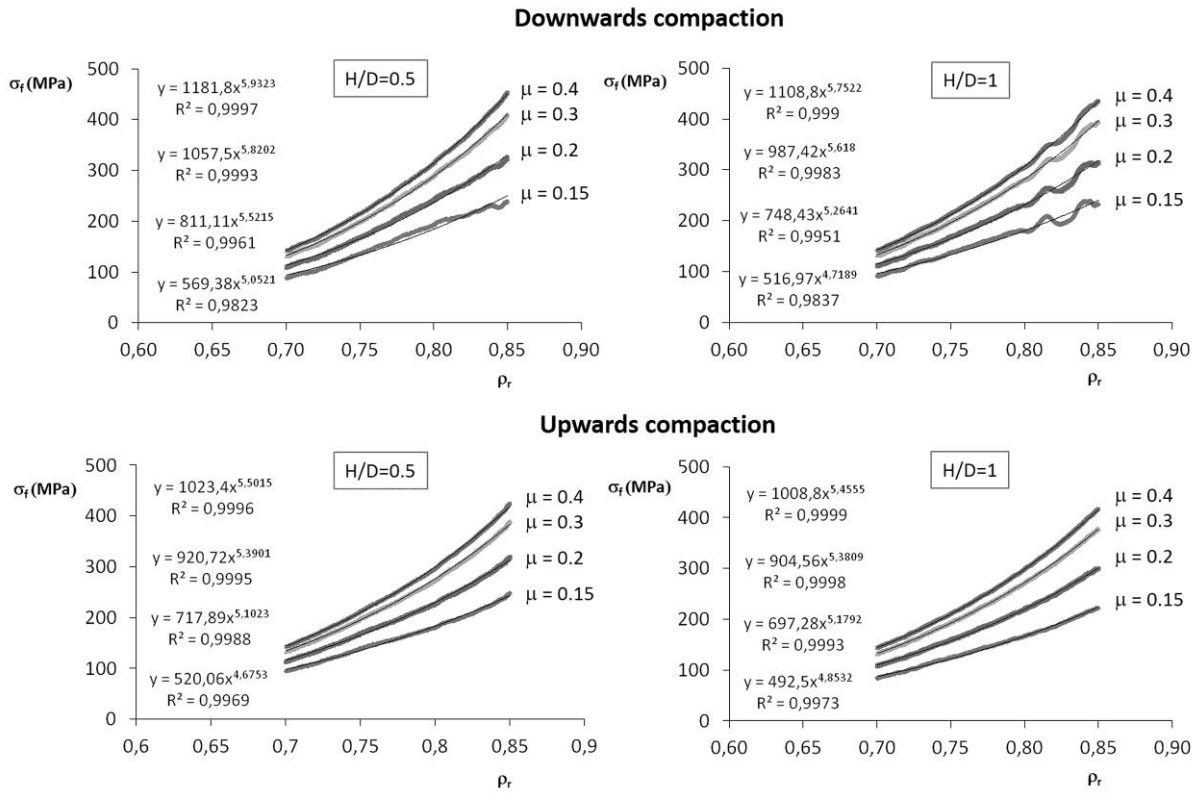


Fig. 12

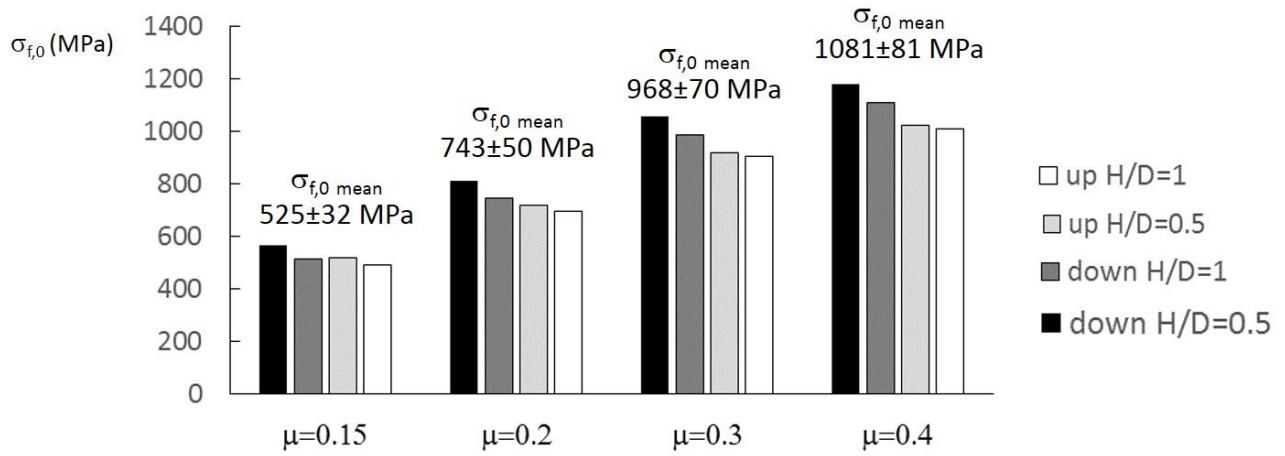


Fig. 13

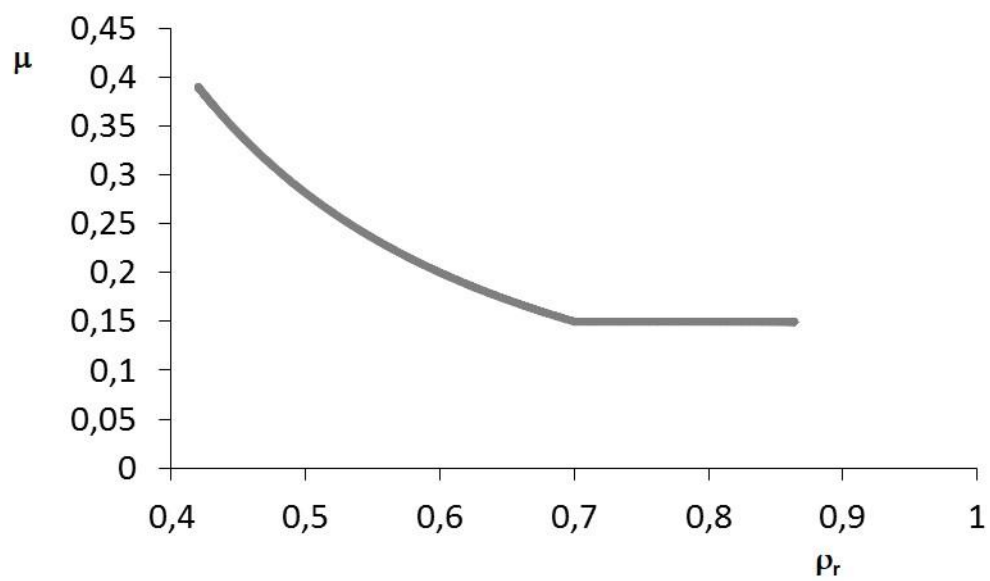


Fig. 14

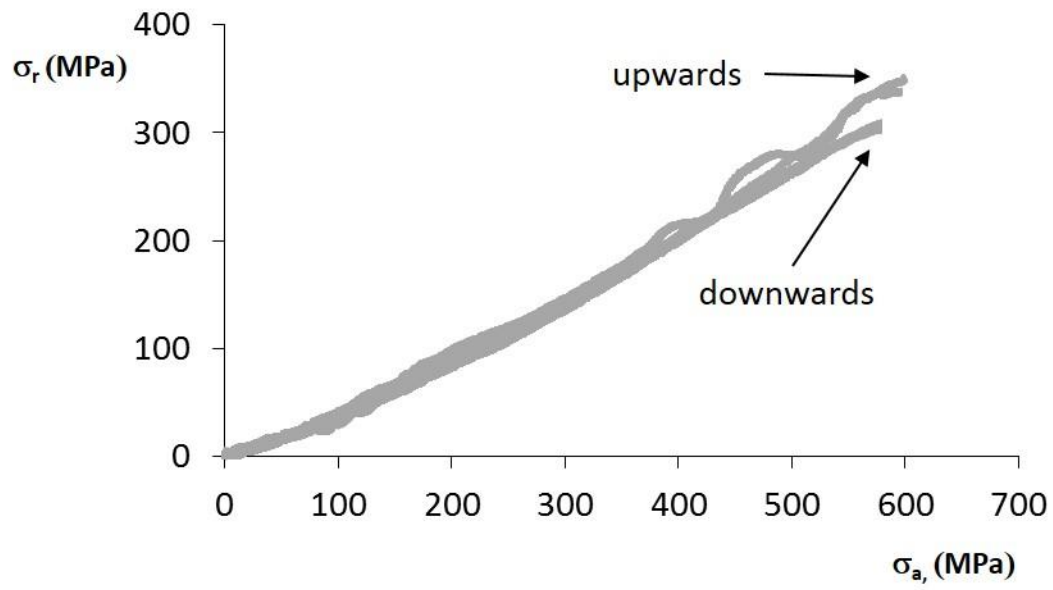


Fig. 15

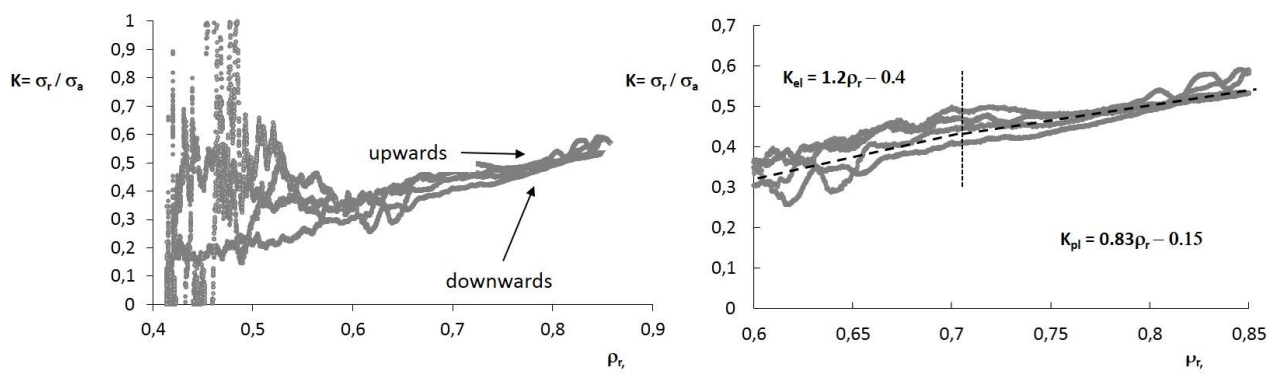


Fig. 16

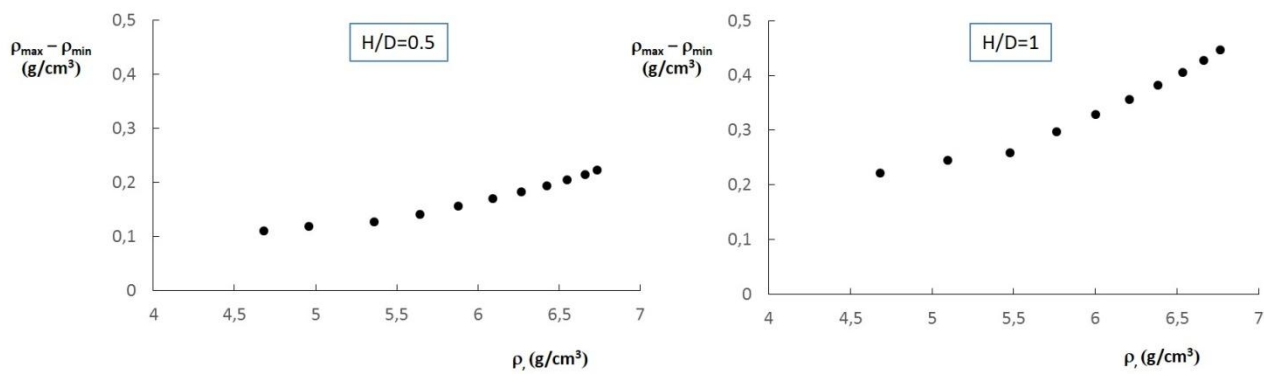
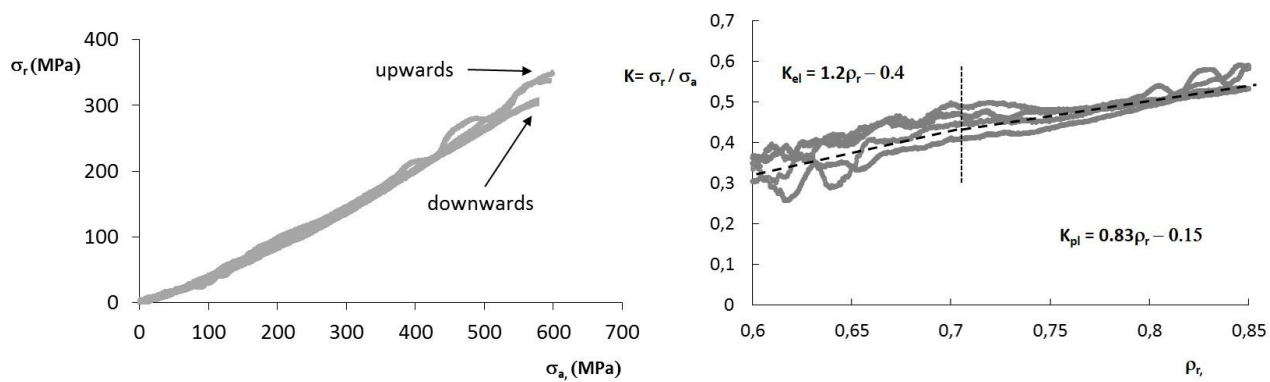


Fig. 17

## Graphical abstract



ACCEPTED MANUSCRIPT

## Research highlights

1. Data recorded by the industrial press were elaborated to investigate the powder behavior
2. The friction coefficient between powder mix and die wall was determined
3. The flow stress vs. relative density was determined
4. The radial and axial stress vs. relative density was determined
5. The radial stress transmission coefficient vs. relative density was determined